

CrystEngComm

Accepted Manuscript



This is an *Accepted Manuscript*, which has been through the Royal Society of Chemistry peer review process and has been accepted for publication.

Accepted Manuscripts are published online shortly after acceptance, before technical editing, formatting and proof reading. Using this free service, authors can make their results available to the community, in citable form, before we publish the edited article. We will replace this *Accepted Manuscript* with the edited and formatted *Advance Article* as soon as it is available.

You can find more information about *Accepted Manuscripts* in the [Information for Authors](#).

Please note that technical editing may introduce minor changes to the text and/or graphics, which may alter content. The journal's standard [Terms & Conditions](#) and the [Ethical guidelines](#) still apply. In no event shall the Royal Society of Chemistry be held responsible for any errors or omissions in this *Accepted Manuscript* or any consequences arising from the use of any information it contains.

Rapid growth of high quality perovskite crystal by solvent mixing

Yangyang Zhou,¹ Tiankai Zhang,² Chunmei Li,¹ Zhimin Liang,¹ Li Gong,³ Jian Chen,³ Weiguang Xie,^{1*} Jianbin Xu,^{2*} Pengyi Liu^{1*}

1. Siyuan Laboratory, Guangzhou Key Laboratory of Vacuum Coating Technologies and New Energy Materials, Department of Physics, Jinan University, Guangzhou, Guangdong 510632, China.
2. Department of Electronic Engineering and Materials Science and Technology Research Center, The Chinese University of Hong Kong, Hong Kong SAR, 999077, P. R. China
3. Instrumental Analysis & Research Center, Sun Yat-sen University, Guangzhou 510275, P. R. China

High quality polycrystalline $\text{CH}_3\text{NH}_3\text{PbI}_3$ was prepared by dripping the γ -butyrolactone (GBL) solution of $\text{CH}_3\text{NH}_3\text{PbI}_3$ into toluene, dimethylformamide (DMF) and dimethylsilicone oil respectively. In toluene, compact $\text{CH}_3\text{NH}_3\text{PbI}_3$ thin film was observed but with grain size smaller than 1 μm because of the rapid extraction of GBL. As $\text{CH}_3\text{NH}_3\text{PbI}_3$ is also soluble in DMF, the crystallization in DMF is understood by interdiffusion induced local and temporal supersaturation droplets, which allow for growth of irregular, separated single crystals with size of more than 0.1 mm. In dimethylsilicone oil, compact, yolk-like polycrystalline $\text{CH}_3\text{NH}_3\text{PbI}_3$ was observed. Unlike the round grain observed in toluene, it is composed of single crystal grains with clear angular surface. The average crystal size is tens of μm and can be modulated by the solvent temperature. We suggest that the poor miscibility between GBL and dimethylsilicone oil, and the poor solubility of $\text{CH}_3\text{NH}_3\text{I}$, PbI_2 and $\text{CH}_3\text{NH}_3\text{PbI}_3$ in the dimethylsilicone oil, allow slow extraction of GBL while keeping the stoichiometric of $\text{CH}_3\text{NH}_3\text{PbI}_3$. The results offer a feasible and high-yield method for growing uniform $\text{CH}_3\text{NH}_3\text{PbI}_3$ crystals in a few seconds.

* Author to whom correspondence should be addressed: W G Xie: wgxie@email.jnu.edu.cn; J B Xu: jbxu@ee.cuhk.edu.hk; P Y Liu: tlpy@jnu.edu.cn;

1. Introduction

Organic lead trihalide perovskite materials (OTP) have attracted great interests due to its excellent photo-electric properties such as high absorption coefficient^{1,2}, long diffusion length^{3,4}, high mobility⁴⁻⁶ and so on. It's found that the above properties are greatly influenced by the crystallinity and the morphology of OTP. Large size, highly crystallized OTP is essential for high performance optoelectronic devices because of longer carrier diffusion length and lower defect density.^{7,8} Single crystal based optoelectronic devices may be more promising to be commercialized in applications than thin film.^{9,10} There are several methods for preparing perovskite large single crystals including top-seed solution growth (TSSG) method,⁷ anti-solvent vapor-assisted crystallization (AVC),¹¹ inverse temperature crystallization^{12,13} and so on. Growth of a two-inch-sized $\text{CH}_3\text{NH}_3\text{PbI}_3$ single crystal was demonstrated by seed-induced growth by Y Liu et al.¹⁴ However, the growth of large single crystal is still too time-consuming and low yield to meet the requirement of mass production.

Application of thin film is restricted by the poor crystallinity and uniformity in large scale.¹⁵ In recent year, solvent engineering is proposed to effectively suppress the growth of grains^{16,17}, leading to uniform thin film for centimeter scale device¹⁸. The solvent engineering is first demonstrated by N J Jeon et al.¹⁶ The $\text{CH}_3\text{NH}_3\text{Pb}(\text{I}_{1-x}\text{Br}_x)_3$ in a mix solution of γ -butyrolactone (GBL) and dimethylsulphoxide (DMSO) was first spin-coated, followed by adding toluene droplet and further extraction of DMSO molecules by annealing.¹⁶ The as-prepared thin film is compact and uniform. In the solvent engineering, the solvent properties are especially important. K Zhu and coworkers suggested 3 rules for the growth of uniform and dense perovskite layers.¹⁷ First, the precursor polar solvent must have high solubility for perovskite and a high boiling point, normally, GBL, DMSO, dimethylformamide (DMF), or N-methyl-2-pyrrolidone (NMP) is used. Second, the extracting solvent, also called anti-solvent should have no solubility and reactivity for the perovskite precursors and the solid perovskite. It should have a low boiling point allowing rapid drying in the ambient. Third, the precursor solvent and the anti-solvent must be highly miscible, inducing supersaturation in the precursor solution in a short time. In the study of M Xiao et al., a series of anti-solvent are investigated.¹⁹ They found that toluene, benzene, xylene and chlorobenzene (CBZ) are suitable to prepare compact and uniform perovskite films, however, with small grain size of hundreds of nanometer.¹⁹ Studies by other groups using the same method show single crystal grain with similar size, implying the limitation of the method.²⁰

Although the aim of the rules is to guide the preparation of high quality thin film, the 2nd and 3rd rules are also applicable in the growth of single crystal. AVC method is developed to growth large OTP single crystal using solvent engineering principle. It's found that the application of dichloromethane (DCM), which is miscible to the precursor solvent (3rd rule) but insoluble to MAPbX_3 , MAX and PbX_2 (2nd rule), strongly improved the quality of crystals and the volumes to more than 100 cubic millimeters.¹¹ To grow larger crystal, a slower growth process is required, which is a little different to the above 3rd rule. In the work of M Xiao et al., the anti-solvent quickly dissolves into the DMF precursor, which reduces the crystallization time. This may be the reason of small crystal size.¹⁹ Therefore, the solvent interaction can be further investigated beyond the above three rules, and we expect that flexible control over the uniformity, size, and morphology of the crystal can be realized.

In this study, we investigate the crystallization of OTP by mixing the precursor solution into different types of solvents. GBL is used as the precursor solvent for $\text{CH}_3\text{NH}_3\text{PbI}_3$. Different to the 2nd rule, we use DMF or DMSO as the second solvent. Both are good solvents for $\text{CH}_3\text{NH}_3\text{PbI}_3$. Different to the 3rd rule, dimethylsilicone oil is used as the second solvent. It has much lower miscibility in GBL than toluene. It is also a poorer solvent to $\text{CH}_3\text{NH}_3\text{PbI}_3$, $\text{CH}_3\text{NH}_3\text{I}$, and PbI_2 than Toluene. The boiling points of all the above solvent are higher than 150 °C, which we expect to increase the crystallization time. Toluene is in common used in the former solvent engineering, and used for comparison here. We find that large scale, well crystallized $\text{CH}_3\text{NH}_3\text{PbI}_3$ can be grown after the above modification. The mechanism responsible for the crystallization process is proposed. The findings enrich our understanding of solvent engineering. This novel approach also enables rapid growth of high-quality MAPbI_3 crystal with high yield.

2. Results & discussion

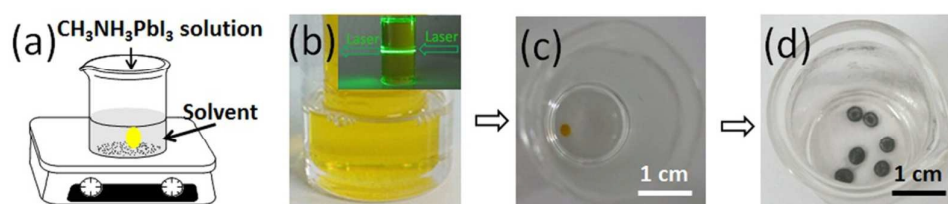


Figure 1 (a) Experimental set-up, (b) $\text{CH}_3\text{NH}_3\text{PbI}_3$ precursor solution, the inset indicates that the solution shows Tyndall effect. (c)-(d) Perovskite crystallization process in dimethylsilicone oil.

Figure 1 shows the schematic of the growth method. The as prepared perovskite solution in **Figure 1(b)** shows a strong Tyndall effect, indicating that the solution has many colloidal particles between room temperature and 150 °C.^{12, 21} These colloidal particles are beneficial to the growth of $\text{CH}_3\text{NH}_3\text{PbI}_3$ crystals. A droplet of perovskite solution was dripped into the second solvent (**Figure 1(c)**). For dimethylsilicone oil, the solvent was kept at 70 °C. For DMF or DMSO, the solvent was kept at 150 °C. Toluene can be kept at room temperature. In order to avoid the inverse crystallization effect, the temperature of the perovskite solution is no less than the temperature of the corresponding second solvent. After the perovskite droplet was dripped into the second solvent, it quickly grew yellow and then turned black (**Figure 1(c) & (d)**). Except in the dimethylsilicone oil, the perovskite droplet quickly dispersed at the bottom of the beaker. In the dimethylsilicone oil, the perovskite droplet kept the droplet shape, and turned black.

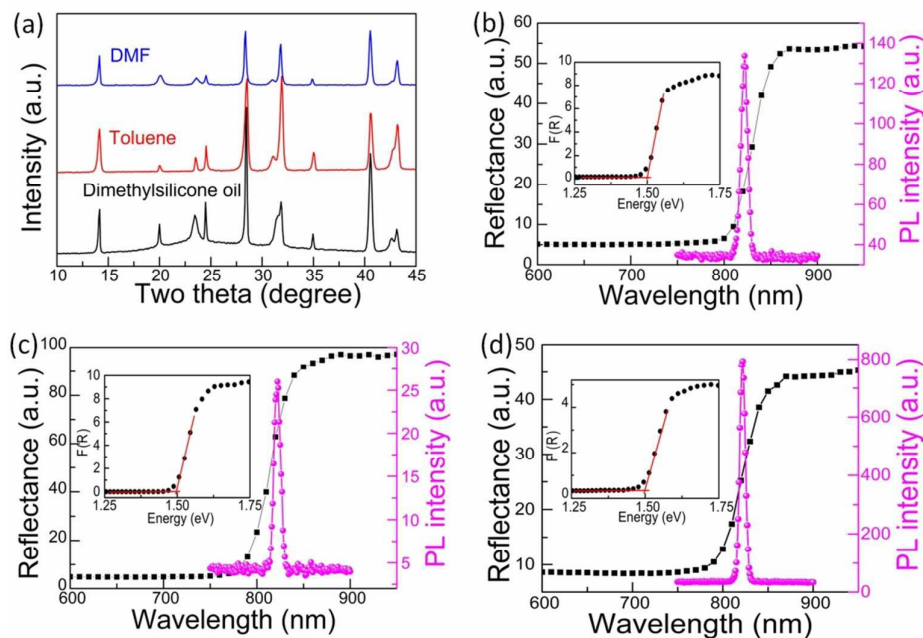


Figure 2 (a) XRD spectra of the CH₃NH₃PbI₃ prepared in different solvents. Reflectance spectra and photoluminescence spectra of the as-prepared CH₃NH₃PbI₃ in DMF (b), toluene (c), and in dimethylsilicone oil (d). The insets show the corresponding Kubelka-munk relations calculated from the reflectance spectra.

The black precipitates were quickly taken out of the solvent and dried for analysis. X-ray diffraction (XRD) spectra in **Figure 2(a)** show that all the precipitates are CH₃NH₃PbI₃ in tetragonal structure.¹¹ A preferential growth direction along [110] direction can be determined. In the sample prepared in dimethylsilicone oil, a small broad background signal centered at ~23° is observed which can be removed by vacuum annealing at 70 °C. We attribute the background to the residue of dimethylsilicone oil because it has high boiling point. However, we can find that the (110) and (220) peaks of the sample shows narrower full-width half maximum (FWHM) and higher intensity, indicating that it has better crystallinity. UV-visible reflectance spectrum is used to measure the band gap of the samples (**Figure 2(b)-(d)**). According to the Kubelka-munk equation, $F(R)=\alpha=(1-R)^2/(2R)$, where R represents the reflectance (%). The band gap can be calculated from the reflectance edge of the F(R)-Energy curves (insets in **Figure 2(b)-(d)**). All the samples show similar value of 1.50 eV, agree with the reported value.²² In addition to the band gap, the photoluminescence spectra of all the samples showed same emission peaks at 820 nm when excitation wavelength is 545 nm. These are consistent with the values of the reported data by using anti-solvent vapor-assisted crystallization.²³ It's found that the PL peak intensity is the strongest in the sample prepared by dimethylsilicone oil, which further support that the sample has better crystallinity than the other two.

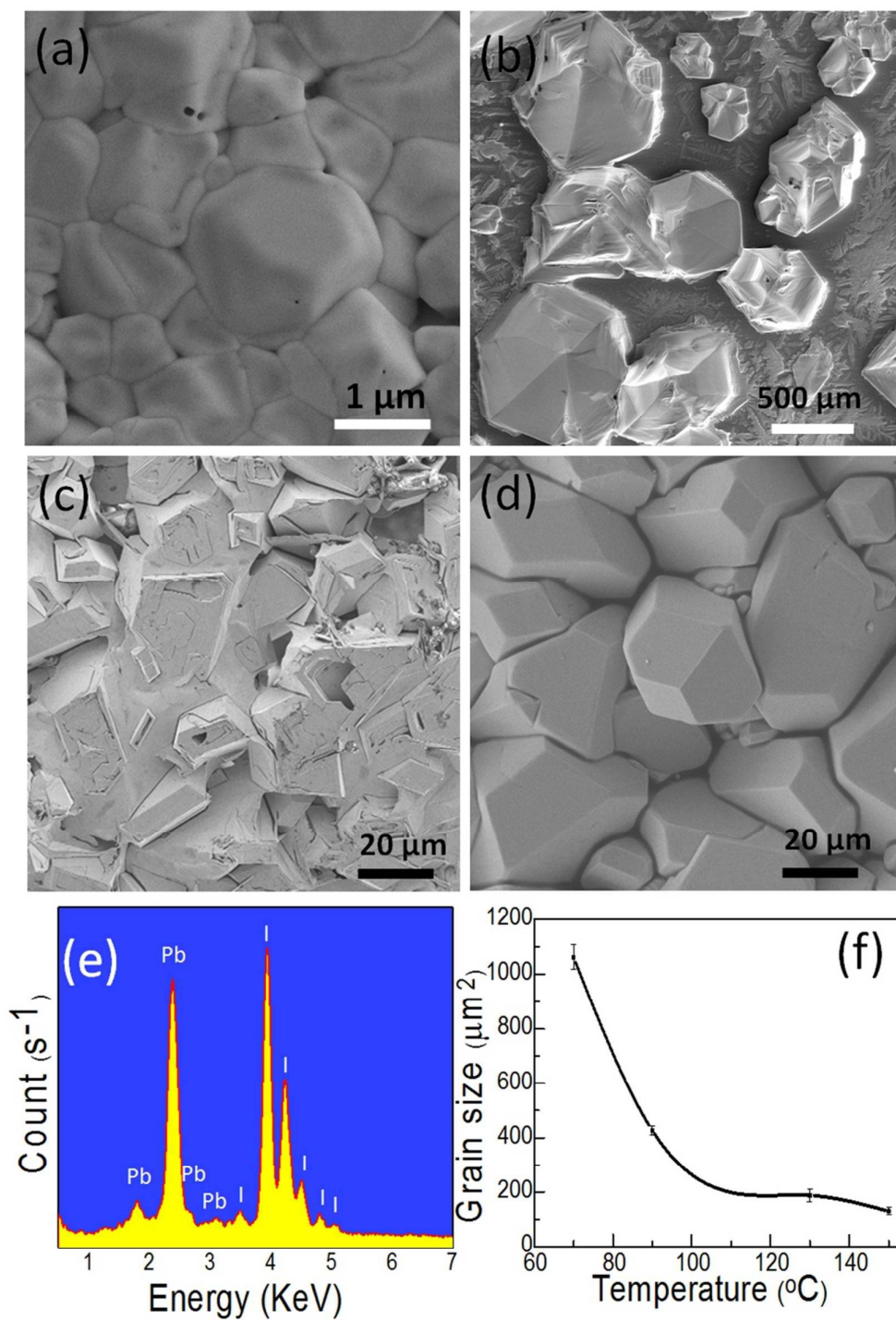


Figure 3 SEM images of $\text{CH}_3\text{NH}_3\text{PbI}_3$ crystallized in toluene (a), DMF (b), and dimethylsilicone oil (c) & (d). (e) EDS spectrum of a $\text{CH}_3\text{NH}_3\text{PbI}_3$ crystal prepared in dimethylsilicone oil. (f) Decrease of crystal area with the temperature of dimethylsilicone oil.

The as-prepared $\text{CH}_3\text{NH}_3\text{PbI}_3$ from toluene shows uniform and compact morphology with small polygon grain size around hundreds of nanometers (**Figure 3(a)**). It's consistent with the results from other groups.^{17, 19, 20} In former study, the process of the anti-solvent approach using toluene is explained

by the schematic in **Figure 4**. Once the toluene is mixed with the $\text{CH}_3\text{NH}_3\text{PbI}_3$ solution, the GBL is extracted quickly to achieve a supersaturation condition, leading to fast crystallization of $\text{CH}_3\text{NH}_3\text{PbI}_3$. The crystallization process in toluene is only a few seconds. The colloidal particles have not enough time to recrystallize, resulting in small crystal grains in the thin film. In addition, the $\text{CH}_3\text{NH}_3\text{I}$ still has a small solubility in toluene, so we observed a poor crystallized surface. As a result, the sample shows the smallest PL intensity shown in **Figure 2(c)**. It explained why excess $\text{CH}_3\text{NH}_3\text{I}$ was required to improve the quality of the thin film.¹⁸

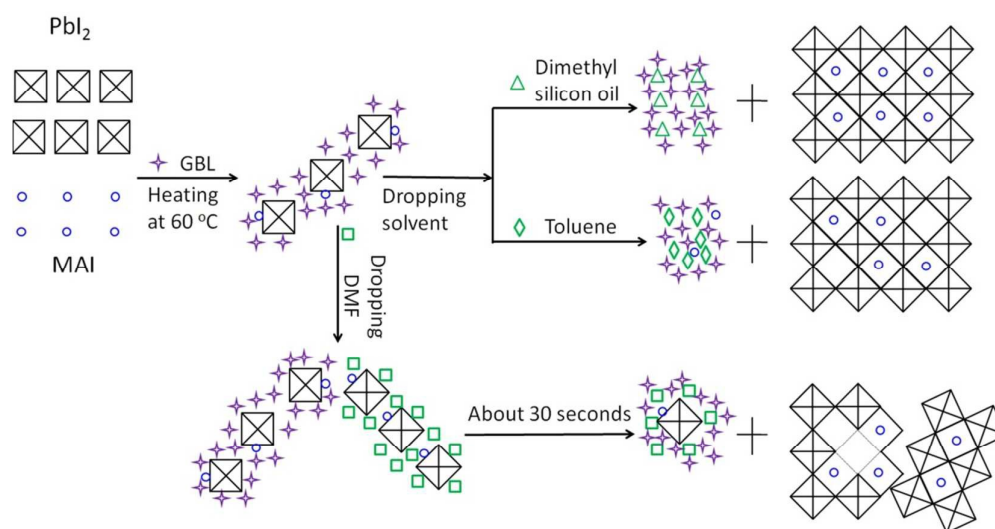


Figure 4 Schematic of the crystal process in the three types of solvent

Largest crystals with typical dimension more than 0.1 mm were found in the DMF solvent (**Figure 3(b)**). DMF is a good solvent for $\text{CH}_3\text{NH}_3\text{PbI}_3$. The observed crystallization of large $\text{CH}_3\text{NH}_3\text{PbI}_3$ means that the 2nd rule is not strict. It's found that the crystals disperse separately, and the crystal shape was irregular. We can also find that some smaller crystals merge together. We suggest that the irregular shape should come from independent nucleation of smaller crystal with different growth direction. When DMF was added into perovskite solution, on one hand, GBL can be extracted from the perovskite solution. On the other hand, the $\text{CH}_3\text{NH}_3\text{PbI}_3$ can also diffuse into DMF. The first process is faster than the second one. A temporal transition zone appears at the interface. There forms a mixture of $\text{CH}_3\text{NH}_3\text{PbI}_3$ droplets with GBL or DMF as solvent. It may induce temporal local supersaturation condition in the droplets. Non-uniform recrystallization takes place separately in droplet, with different crystallization rate and crystal orientation, so large irregular crystals were observed.

Unlike the above crystallization, the perovskite solution does not disperse in the dimethylsilicone oil. Therefore, a yurt-like structure was observed after crystallization (**Figure 1(d)**). Dimethylsilicone oil and GBL are immiscible at room temperature, and we found no precipitates at room temperature even after several days. It means that the 3rd rule takes effect. However, with increasing temperature, the GBL was found to slightly diffuse into the dimethylsilicone oil, which can be used to control the crystallization process. Crystallization was found when the temperature was around 50-70 °C. The crystallization can be understood as shown in **Figure 4**. During the diffusion of GBL into the dimethylsilicone oil, the solutes are carried to the liquid interface. The dimethylsilicone oil is still

immiscible to $\text{CH}_3\text{NH}_3\text{I}$, PbI_2 and $\text{CH}_3\text{NH}_3\text{PbI}_3$ at high temperature, the $\text{CH}_3\text{NH}_3\text{PbI}_3$ will nucleate and deposit on the surface of dimethylsilicone oil. As a result, a compact crystal surface plane appears at the outer surface of the yurt-like structure (**Figure 3(c)**). On the inner surface, we can find that it's composed of crystal grains with average area of $\sim 10^3 \mu\text{m}^2$ (**Figure 3(d)**). Both surfaces show clear and uniform crystallographic plane because the solvents are not lost, which is consistent with the stronger XRD peak intensity and narrower FWHM in **Figure 2(a)**. **Figure 3(e)** presents the EDS analysis of the crystal. The atomic ratio of I and Pb is 3.01, complying with the chemical composition in $\text{CH}_3\text{NH}_3\text{PbI}_3$.

Increasing the temperature is able to enhance the extraction of GBL, which provides the possibility to control the size of grains. **Figure 3(f)** shows that the average crystal area decreases from $1062.6 \mu\text{m}^2$ to $130.2 \mu\text{m}^2$ when the temperature increases from $70 \text{ }^\circ\text{C}$ to $150 \text{ }^\circ\text{C}$. A faster crystallization speed can be observed as temperature increases. The result indicates that fast extraction of GBL may be not an essential condition for the growth of compact thin film. Increasing the grains size by increasing the crystallization time can be applicable. The requirement of fast crystallization may be due to the small solubility of $\text{CH}_3\text{NH}_3\text{I}$ in toluene and other solvent used in former studies. A slower crystallization process will lead to decomposition of the $\text{CH}_3\text{NH}_3\text{PbI}_3$ due to the loss of $\text{CH}_3\text{NH}_3\text{I}$. Therefore, further studies should focus on finding a solvent with ultra-poor solubility to $\text{CH}_3\text{NH}_3\text{I}$, PbI_2 and $\text{CH}_3\text{NH}_3\text{PbI}_3$.

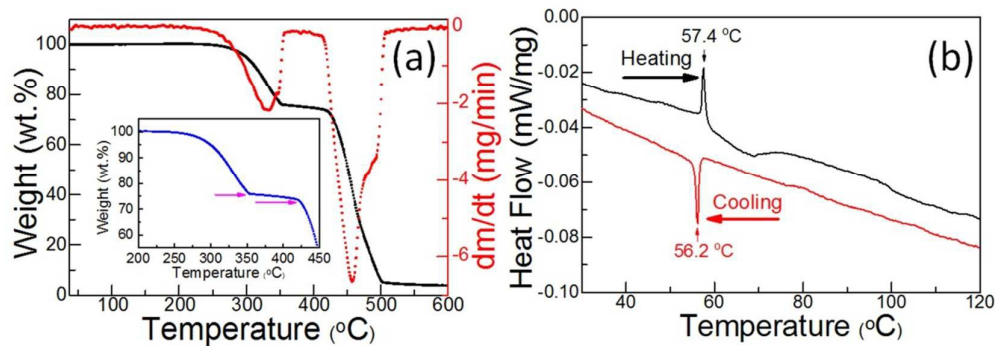


Figure 5 Thermogravimetric (TG) curve (a) and differential scanning calorimeter (DSC) plot (b) for MAPbI_3 prepared in dimethylsilicone oil.

The as prepared perovskite keeps black when stored in air for several days. To further investigate the stability of $\text{CH}_3\text{NH}_3\text{PbI}_3$ single crystals, the thermogravimetric (TG) and differential scanning calorimeter (DSC) curves were shown in **Figure 5 (a) & (b)**. **Figure 5(a)** indicates that the samples are stable up to $240 \text{ }^\circ\text{C}$. On the other hand, when the temperature rises from room temperature to $500 \text{ }^\circ\text{C}$, the samples exhibit two thermal events. Material first undergoes 20% weight loss at $343 \text{ }^\circ\text{C}$, indicating a loss of HI, and followed by another 6% mass loss of CH_3NH_2 component at $415 \text{ }^\circ\text{C}$.¹⁴ The results demonstrate that amine group can be more firmly bound to perovskite structure comparing to HI. As many $\text{CH}_3\text{NH}_3\text{PbI}_3$ materials decompose at about $150 \text{ }^\circ\text{C}$,^{24, 25} the as prepared $\text{CH}_3\text{NH}_3\text{PbI}_3$ crystals exhibit better stability. The DSC curve in **Figure 4(b)** shows that during heating process, the phase transition temperature from tetragonal to cubic structure is $57.4 \text{ }^\circ\text{C}$. In the cooling process, the transition temperature is $56.2 \text{ }^\circ\text{C}$. This is consistent with the relevant reports.^{26, 27} The above results show that the crystal has good structural, optical properties and thermal stability. Although the size of

single crystal grain cannot reach 1 mm, we find that the yield of crystallization is above 70%, higher than the former reported 11%.¹³ Therefore, it's a feasible and rapid method to grow large scale, high quality $\text{CH}_3\text{NH}_3\text{PbI}_3$ polycrystalline structure with controllable grains size.

Conclusion

In conclusion, we have compared the growth of MAPbI_3 in three different types of solvents using solvent mixing method. The results show the crystal structure and size are controlled by the interdiffusion behavior of the two solvents. Dimethylsilicone oil is the best solvent for rapid growth of high quality, compact perovskite polycrystals. The size of the crystal can be controlled by the solvent temperature. The findings enrich our understanding of solvent engineering in the preparation of high quality perovskite crystals. It provides a feasible way for rapid growth of perovskite crystals and method to control the crystal size.

Methods

The synthesis of $\text{CH}_3\text{NH}_3\text{PbI}_3$ single crystals. Equimolar $\text{CH}_3\text{NH}_3\text{I}$ (>99.8%) and PbI_2 (99%) were mixed in 2.5 ml GBL (>99.8%), and stirring on the hotplate set at 60°C. After perovskite completely dissolving in GBL, 5 μl perovskite solution was dripped into the second solvent (dimethylsilicone oil, DMF or toluene) with volume of 1 ml. All procedures were completed under ambient conditions, with temperature at 25°C and humidity of 55% to 65%.

Measurement and characterization. The X-ray diffraction (XRD) pattern was measured in a Rigaku-MiniFlex600 using the $\text{Cu K}\alpha$ radiation (1.546 Å), with voltage of 40kV and current of 40 mA. The Enlitech's QE-R system was used to measure UV-visible spectrum. The photoluminescence spectrum was performed on Shimadzu RF-5301PC. The morphology and EDS of $\text{CH}_3\text{NH}_3\text{PbI}_3$ were characterized by Zeiss Ultra 55 scanning electron microscope (SEM). Thermo gravimetric and differential scanning calorimeter were carried out on Netzsch TG209 F1 and DSC-204 F1 at constant N_2 flow of 50ml/min with heating and cooling rates of 5 °C/min. The grain size is measured by calculating the area of a single crystal grain from the SEM image.

ACKNOWLEDGEMENTS

This work is in part supported by the National Natural Science Foundation of China (Grants Nos. 11574119, 51373205), the Guangdong Natural Science Foundation (Grants Nos. 2014A030313381), and the Research Grants Council of Hong Kong (Grant Nos. AoE/P-03/08, N_CUHK405/12, T23-407/13-N, AoE/P-02/12, CUHK1/CRF/12G,14207515).

Reference

1. H.-S. Kim, J.-W. Lee, N. Yantara, P. P. Boix, S. A. Kulkarni, S. Mhaisalkar, M. Grätzel and N.-G. Park, *Nano Lett.*, 2013, **13**, 2412-2417.
2. G. Xing, N. Mathews, S. Sun, S. S. Lim, Y. M. Lam, M. Grätzel, S. Mhaisalkar and T. C. Sum, *Science*, 2013, **342**, 344-347.

3. J. Huang, Y. Shao and Q. Dong, *The Journal of Physical Chemistry Letters*, 2015, **6**, 3218-3227.
4. Q. Dong, Y. Fang, Y. Shao, P. Mulligan, J. Qiu, L. Cao and J. Huang, *Science*, 2015, **347**, 967-970.
5. C. C. Stoumpos, C. D. Malliakas and M. G. Kanatzidis, *Inorganic Chemistry*, 2013, **52**, 9019-9038.
6. C. Wehrenfennig, G. E. Eperon, M. B. Johnston, H. J. Snaith and L. M. Herz, *Adv. Mater.*, 2014, **26**, 1584-1589.
7. Q. Dong, Y. Fang, Y. Shao, P. Mulligan, J. Qiu, L. Cao and J. Huang, *Science*, 2015, **347**, 967-970.
8. W. Tian, C. Zhao, J. Leng, R. Cui and S. Jin, *J. Am. Chem. Soc.*, 2015, **137**, 12458-12461.
9. H. Zhu, Y. Fu, F. Meng, X. Wu, Z. Gong, Q. Ding, M. V. Gustafsson, M. T. Trinh, S. Jin and X. Y. Zhu, *Nat Mater*, 2015, **14**, 636-642.
10. Y. Fu, F. Meng, M. B. Rowley, B. J. Thompson, M. J. Shearer, D. Ma, R. J. Hamers, J. C. Wright and S. Jin, *J. Am. Chem. Soc.*, 2015, **137**, 5810-5818.
11. D. Shi, V. Adinolfi, R. Comin, M. Yuan, E. Alarousu, A. Buin, Y. Chen, S. Hoogland, A. Rothenberger, K. Katsiev, Y. Losovyj, X. Zhang, P. A. Dowben, O. F. Mohammed, E. H. Sargent and O. M. Bakr, *Science*, 2015, **347**, 519-522.
12. J. M. Kadro, K. Nonomura, D. Gachet, M. Grätzel and A. Hagfeldt, *Sci. Rep.*, 2015, **5**, 11654.
13. M. I. Saidaminov, A. L. Abdelhady, B. Murali, E. Alarousu, V. M. Burlakov, W. Peng, I. Dursun, L. Wang, Y. He, G. Maculan, A. Goriely, T. Wu, O. F. Mohammed and O. M. Bakr, *Nat Commun*, 2015, **6**, 7586.
14. Y. Liu, Z. Yang, D. Cui, X. Ren, J. Sun, X. Liu, J. Zhang, Q. Wei, H. Fan and F. Yu, *Adv. Mater.*, 2015, 1-8.
15. W. Nie, H. Tsai, R. Asadpour, J.-C. Blancon, A. J. Neukirch, G. Gupta, J. J. Crochet, M. Chhowalla, S. Tretiak, M. A. Alam, H.-L. Wang and A. D. Mohite, *Science*, 2015, **347**, 522-525.
16. N. J. Jeon, J. H. Noh, Y. C. Kim, W. S. Yang, S. Ryu and S. I. Seok, *Nat Mater*, 2014, **13**, 897-903.
17. Y. Zhou, M. Yang, W. Wu, A. L. Vasiliev, K. Zhu and N. P. Padture, *J. Mater. Chem. A*, 2015, **3**, 8178-8184.
18. M. Yang, Y. Zhou, Y. Zeng, C.-S. Jiang, N. P. Padture and K. Zhu, *Adv. Mater.*, 2015, **27**, 1-8.
19. M. Xiao, F. Huang, W. Huang, Y. Dkhissi, Y. Zhu, J. Etheridge, A. Gray-Weale, U. Bach, Y.-B. Cheng and L. Spiccia, *Angewandte Chemie*, 2014, **126**, 10056-10061.
20. X. Zheng, B. Chen, C. Wu and S. Priya, *Nano Energy*, 2015, **17**, 269-278.
21. K. Yan, M. Long, T. Zhang, Z. Wei, H. Chen, S. Yang and J. Xu, *J. Am. Chem. Soc.*, 2015, **137**, 4460-4468.
22. T. Baikie, Y. N. Fang, J. M. Kadro, M. Schreyer, F. X. Wei, S. G. Mhaisalkar, M. Graetzel and T. J. White, *J. Mater. Chem. A*, 2013, **1**, 5628-5641.
23. G. Grancini, V. D'Innocenzo, E. R. Dohner, N. Martino, A. R. Srimath Kandada, E. Mosconi, F. De Angelis, H. I. Karunadasa, E. T. Hoke and A. Petrozza, *Chemical Science*, 2015, **6**, 7305-7310.
24. T. Supasai, N. Rujisamphan, K. Ullrich, A. Chemseddine and T. Dittrich, *Appl. Phys. Lett.*, 2013, **103**.
25. A. Dualeh, N. Tetreault, T. Moehl, P. Gao, M. K. Nazeeruddin and M. Gratzel, *Adv. Funct. Mater.*, 2014, **24**, 3250-3258.
26. J. Su, D. P. Chen and C. T. Lin, *Journal of Crystal Growth*, 2015, **422**, 75-79.
27. T. Baikie, Y. Fang, J. M. Kadro, M. Schreyer, F. Wei, S. G. Mhaisalkar, M. Graetzel and T. J. White, *J. Mater. Chem. A*, 2013, **1**, 5628-5641.

